

Sheila P. Werth\* and Stephen J. Frasier  
University of Massachusetts Amherst, Amherst Massachusetts

## 1. INTRODUCTION

Wind energy is one of the fastest-growing segments of the world energy market, offering a clean and abundant source of electricity to meet growing demands. However, wind energy facilities can have detrimental effects on wildlife, especially birds and bats. Monitoring tools are needed to better quantify the potential and ongoing impacts of wind installations.

Radar monitoring systems based on marine navigation radar are often used to track bird and bat migration near proposed wind sites. Unlike camera and acoustic based methods, radar works at great distances, providing resolved range information. However, the ability to distinguish between bats and different varieties of birds is still not practically achieved. This capability could enable site selection that favors more vulnerable species, such as bats and raptors. Radar signatures of biological targets have been studied using dual polarized weather radars (Cachmann and Zrnic 2008; Melnikov et al. 2014; Stepanian et al. 2014), although primarily for the purpose of preventing contamination of meteorological data. Recent evidence suggests that polarimetric signatures of avian targets have an orientation dependence that differs by species (Stepanian et al. 2014).

This paper explores the broad species-based classification potential of polarimetric and Doppler radar measurements. Section 2 contains a summary of hardware and data collection methods, followed by a brief description of the detection and preprocessing algorithms used (Section 3). Section 4 provides an overview of the two-stage feature extraction and analysis approach. The first stage is a novel technique for determining each birds' instantaneous behavioral state (i.e. flapping/gliding), described in Section 5. When the behavioral state is known, a second set of features is extracted to enable comparison between birds of different species. This process will be covered in Section 6. Preliminary results and broader impacts are reviewed in Section 7.

## 2. DATA COLLECTION PROCEDURE

A dual-polarized X-band mobile Doppler radar ("UMass X-Pol"), shown in Figure 1, was used to collect observations of migrating birds. With 12.5 kW (6.25 kW per polarization) peak transmit power and a narrow 1.25° parabolic dish antenna, the UMass X-Pol radar is sensitive enough to detect birds at ranges as great as 20km.

To collect study data, the radar was parked in a stationary position, looking eastward, with the antenna fixed at ten degrees elevation. Time series in-phase and quadrature channel radar data was logged as birds moved through the stationary beam. Data was collected during clear air conditions in Western, Massachusetts, over ten separate evenings during Fall 2014. The full dataset contains several thousand bird observations of unknown species.

## 3. DETECTION, PREPROCESSING, AND INITIAL FEATURE EXTRACTION

Bird observations were a small subset of the hundreds of gigabytes of original unprocessed radar data. To extract just observations of interest, ground clutter was removed and raw data were coherently integrated to improve the signal-to-noise ratio. Local maxima, exceeding an SNR threshold, were detected in the range-time domain. A detected bird would be present in the beam for an extended time, so power at times around each local maximum were summed and compared to a second threshold. Observations exceeding the second threshold were classified as bird detections and added to the filtered data set.

Standard meteorological polarimetric products, including differential reflectivity  $Z_{dr}$ , correlation coefficient  $\rho_{hv}$ , and differential phase  $\psi_{dp}$  were computed for each bird, at each time step over the duration of the observation. Differential reflectivity  $Z_{dr}$ , a measure of target aspect ratio, is the ratio of reflectivity at horizontal polarization  $Z_h$  to reflectivity in the vertical polarization  $Z_v$ .

$$Z_{dr} = 10 * \log\left(\frac{Z_h}{Z_v}\right) \quad (1)$$

Correlation coefficient  $\rho_{hv}$  is a measure of the similarity between both polarizations of the received echo voltages ( $E_h$  and  $E_v$ ):

---

\* Corresponding author address: Sheila P. Werth, Univ. of Massachusetts Amherst, Dept. of Electrical and Computer Engineering, Amherst, MA 01002; e-mail: [sheila.werth@gmail.com](mailto:sheila.werth@gmail.com)

$$\rho_{hv} = \frac{|\langle E_h E_v^* \rangle|}{\sqrt{\langle |E_h|^2 \rangle \langle |E_v|^2 \rangle}} \quad (2)$$

Differential phase  $\psi_{dp}$  is the difference between H-polarized and V-polarized echo phase, and is a measure of target shape.

$$\psi_{dp} = \psi_h - \psi_v = \angle \langle E_h E_v^* \rangle \quad (3)$$

In addition to extracting polarimetric features, a horizontally and vertically polarized Doppler spectrogram was produced for each bird. The spectrogram shows the way in which the Doppler spectrum changes in time, including torso speed and micro-Doppler signatures associated with moving parts around the torso (i.e. flapping).

If the total received signal at the radar, for a single range bin, is given by  $rx(n)$ , where  $n$  is the sample index, the Doppler spectrogram  $sg(w, t)$  of this signal is:

$$sg(w, t) = \left| \sum_{q=0}^{Q-1} Ham(q) * rx(q + (t-1)(Q-M)) * e^{\frac{j2\pi wq}{Q}} \right|^2 \quad (4)$$

where  $M$  is the length of overlap in the time series', of length  $Q$ , used to produce each subsequent spectrum,  $Ham(q)$  is the Hamming window function,  $w$  denotes frequency filter bin, and  $t$  is the time stamp corresponding to each spectrum. Micro-Doppler features are isolated by normalizing the bird's torso velocity to the zero-velocity frequency bin in the spectrogram image.

#### 4. FEATURE EXTRACTION APPROACH

When a bird is engaging in different behaviors (i.e. flapping/gliding states), its body shape and orientation change, causing it to appear differently to the radar. Figure 1 shows how Doppler and polarimetric features change in time as one bird cycles through behavioral states. For the bird shown in Figure 1, gliding behavior is characterized by small spectrum width (A), lower H-polarized return power (B), and high correlation coefficient (C). Lower and more static values of differential reflectivity (D) are also observed. These trends differ by species and orientation.

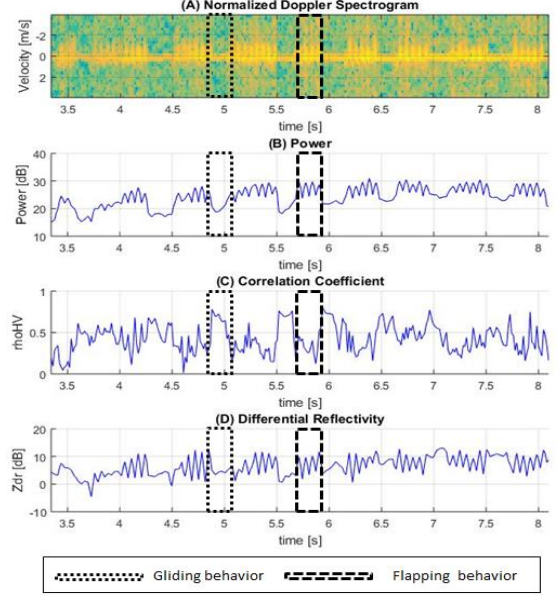


Figure 1 – Time changing radar signatures for a single bird observation are different during flapping and gliding behaviors. (A) Normalized Doppler spectrogram for H-polarization, (B) H-polarization echo power in [dB], (C) correlation coefficient  $\rho_{hv}$ , and (D) differential reflectivity in [dB]

In order to evaluate parameters for species-based classification potential, two feature extraction stages are used (shown in Figure 2). The *first feature space* contains the time-dependent polarimetric and Doppler features described in Sections 3.1-3.2. As shown in Figure 1, these features change in time, and may be mapped to the instantaneous behavioral state of the bird. Determining the behavioral state of a bird at each time step, described in Section 5, yields a second feature space that provides a holistic description of that bird. These features differ by species and include:

- (1) **Temporal Features** – The duration and spacing between different behavioral states. Related to a bird's wingbeat frequency and gliding intervals, summarizing its time changing behavioral patterns. Strong, known, correlation with species (Vaughn 1985).
- (2) **Statistical Features** – Description of how a bird appears to the radar when it is engaging in each behavioral state.

This second feature space enables comparison between birds, and will be described in Section 6.

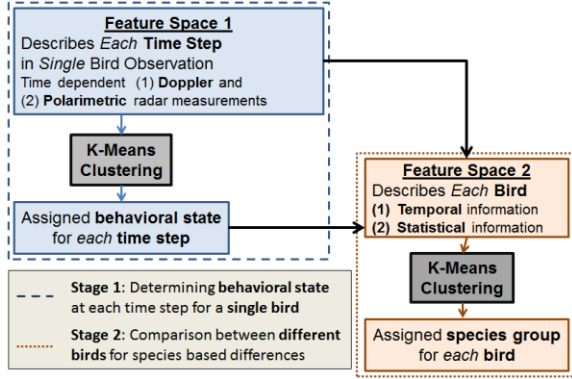


Figure 2 – Two feature spaces are used to assess species based classification potential. The first feature space describes each time step during a single bird observation, enabling those times steps to be assigned to a set of behavioral states. The second feature space is derived from the assigned behavior states, containing temporal and statistical information, and is used to compare between birds.

## 5. STAGE 1: DETERMINING AND CHARACTERIZING BEHAVIORAL STATE

In order to determine the behavioral state of a bird at each time step, the k-means clustering algorithm was used. K-means takes, as arguments, a list of observations, each described by a measurement vector, and sorts them into  $n$  most closely spaced (Euclidian) clusters of observations. In this application, each observation is a time-step defined by a feature vector of polarimetric and Doppler features measured at that given time. These time-step inputs were clustered into  $n = 3$  possible behavioral states: *gliding*, *flapping 1*, and *flapping 2*. A list of features measured at each time includes:

- (1) Reflectivity ( $Z_h$  and  $Z_v$ )
- (2) Differential Reflectivity ( $Z_{dr}$ )
- (3) Correlation Coefficient ( $\rho_{hv}$ )
- (4) Differential Phase ( $\psi_{dp}$ )
- (5) Spectral width ( $\sigma_h$  and  $\sigma_v$ )
- (6) Differential spectral width ( $\sigma_h/\sigma_v$ )
- (7) Doppler bins from spectrogram ( $w_1$  through  $w_Q$ )

In addition to the measurements listed above, the feature vector for each time stamp also included (A) the first derivative of each of these measurements as well as (B) all six measurements at four adjacent time steps (two on each side).

Before applying the k-means clustering algorithm, each feature  $x$  was smoothed using local linear regression to determine local effects of the antenna pattern and normalized accordingly:

$$x_{norm} = x - x_{smooth} \quad (5)$$

Features were then rescaled before applying weighting ( $W$ ):

$$x'_{norm} = W * \left( \frac{x_{norm} - \min(x_{norm})}{\max(x_{norm}) - \min(x_{norm})} \right) \quad (6)$$

Sample behavioral clustering results are shown in Figure 3C, for the same bird observation described in Figure 1. Figure 3C shows the behavioral state assigned to each time-step by the k-means clustering algorithm. This particular bird spends extended intervals in behavioral state 1 (*gliding*) and then oscillates between behavioral state 2 (*flapping 1*) and behavioral state 3 (*flapping 2*).

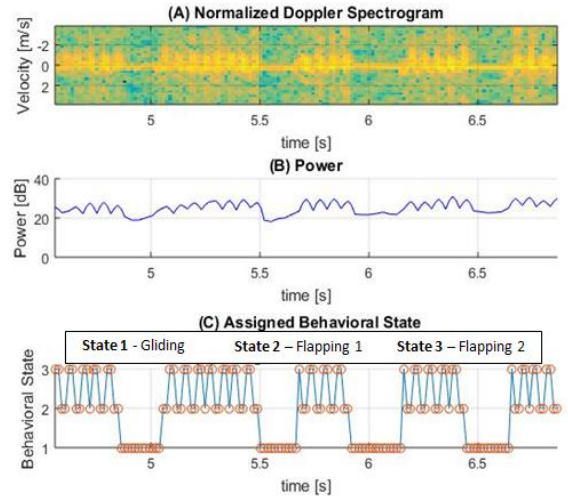


Figure 3 – Same bird as Figure 1. (A) H-Polarized spectrogram, (B) H-polarized echo power, and (C) behavioral state assigned by k-means clustering algorithm. Gliding periods are extended periods of time. During flapping periods, the bird alternates between flapping 1 and flapping 2 as it moves its wings.

Identity was assigned to the k-means output clusters according to the following rules:

- (1) **Cluster 1: Gliding Behavior:** *if* there is a behavioral state that remains active for extended time intervals, as is the case in Figure 3C, then this state is the gliding state. *If* there is no behavioral state with extended active intervals, then the state with the highest average correlation coefficient is determined to be the gliding state.
- (2) **Cluster 2: Flapping 1** is the state, of the remaining two, with the highest average value of spectral width in the vertically polarized channel
- (3) **Cluster 3: Flapping 2** is the state remaining after the first two have been assigned

These rules were selected based upon a review of features containing maximum variance across the sample as well as several radar observations with paired video footage of the corresponding bird in flight. Two possible flapping states exist in order to capture wingbeat temporal information during flapping intervals.

Utility Score	Feature
1	H-Pol Spectrogram Row at $\bar{v} - \Delta v$
2	H-Pol Total Reflectivity
3	V-Pol Spectrogram Row at $\bar{v} - \Delta v$
4	Differential Reflectivity
5	V-Pol Total Reflectivity
6	Differential Spectrum Width
7	H-Pol Spectrogram Row at $\bar{v} - 2\Delta v$
8	V-Pol Spectrogram Row at $\bar{v} - 2\Delta v$
9	V-Pol Spectrogram Row at $\bar{v} + \Delta v$
10	H-Pol Spectrogram Row at $\bar{v} + \Delta v$
11	V-Pol Spectrum Width
12	H-Pol Spectrogram Row at $\bar{v} + 3\Delta v$
13	Correlation Coefficient
14	H-Pol Spectrogram Row at $\bar{v} + 4\Delta v$
15	H-Pol Spectrum Width

**Key:**  $\bar{v}$  is the torso speed, normalized to the center of spectrogram.  $\Delta v$  denotes the width of each Doppler bin in [cm/s].  
*"H-Polarization at  $\bar{v} + n\Delta v$ "* represents a row of the H-polarized spectrogram, offset from the center by  $n$  Doppler bins.

Table 1 – Summary of features, ranked by their measured utility in the behavioral classification process. The most useful fifteen features are listed.

Table 1 contains a list of features, ranked by utility in the behavioral classification process. Features found to be the least useful are excluded from the table. Classification utility was determined using principal component analysis, isolating the features that contribute most to the directions of greatest variance in the data. It should be noted that the table contains aggregate results averaged across all birds; although the most useful polarimetric and Doppler features did differ substantially between bird observations. Spectrogram rows close to the center Doppler bin  $\bar{v}$  were universally useful in classifying behavioral state across all birds, while features like correlation coefficient were extremely useful only in a subset of observations. This variation is reflected in the rankings in Table 1. Physically speaking, spectrogram rows near the center row ( $\bar{v}$ ) represent the return power from components of the bird (i.e. wings) that are moving ( $n \cdot \Delta v$ ) with respect to the

torso ( $\bar{v}$ ). For this reason, their utility in classifying a bird's behavioral state was expected.

## 6. STAGE 2: COMPARING BETWEEN BIRDS OF DIFFERENT SPECIES

Once the behavioral state of a bird has been determined at each time, this information is used to derive a second set of features. Temporal features describe the way that a bird's behavioral state changes in time. Statistical features describe the way that a bird looks to the radar during each behavioral state, in terms of the polarimetric and Doppler measurements. For example; one statistical feature is the average value of correlation coefficient  $\rho_{hv}$  during gliding intervals. As shown in Figure 1, this value may be higher than the value of  $\rho_{hv}$  during flapping intervals. Exactly how much higher is a function of species and orientation.

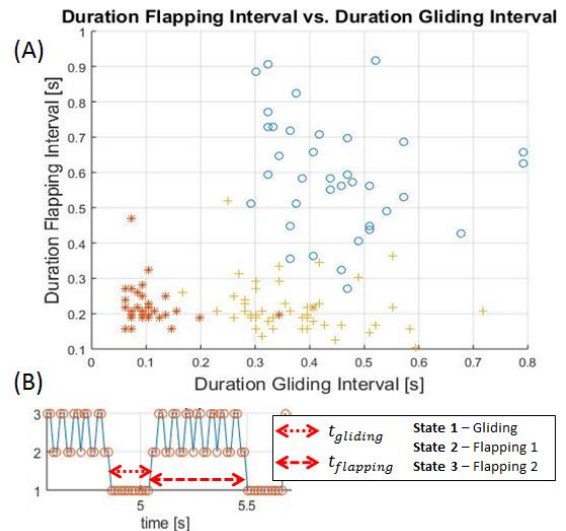


Figure 4 – (A) Bird observations, plotted in terms of their average gliding and flapping intervals, fall into clear groups.

Birds of different species are known to have different flapping and gliding intervals (Vaughn 1985). (B) shows the method used to extract gliding and flapping intervals from the assigned behavioral state.

Temporal and statistical features may be used to compare between birds of different species. Figure 4 shows the distributions of (A) time spent gliding and (B) time spent flapping. Clear clusters of birds, based on temporal behaviors, exist. Work to further subdivide within these groups is in progress. Continued research focuses on evaluating the full set of temporal and statistical features for species based classification potential. Collecting an extensive set of supervised observations, where the species of the bird is known, will be critical in this stage.

## **7. PRELIMINARY CONCLUSIONS**

This paper presents a novel two-stage feature extraction method to enable comparison between birds of different species in radar echoes. The first stage involves determining the behavioral state of a bird at each time stamp, across the duration of the observation. Our method for extracting wing-beat temporal information from these assigned behavioral states is more localized in time and performs better on radar echoes with lower signal-to-noise ratio, compared to conventional Fourier transform based methods. Spectral information extracted from spectrograms and polarimetric measurements proved useful. Preliminary clustering results show clear groups of bird observations with different flapping behavior in time.

Future work will focus on improving characterization of temporal and statistical features by species. This effort will require a more extensive set of ground truth data. The ability to ultimately distinguish between birds of different species in radar returns could transform the wind siting process, allowing site selection that favors more vulnerable species.

## **7. ACKNOWLEDGEMENTS**

This study was supported by National Science Foundation award 1068864 (IGERT: Offshore Wind Energy Engineering, Environmental Science, Policy). I would like to thank Krzysztof Orzel, Thomas Hartley, and Roy Sivley for their help.

## **8. REFERENCES**

Bachmann, S. M, and Zrnic, D S., 2008: Three-dimensional attributes of clear-air scatterers observed with the polarimetric weather radar. *IEEE Geosci. Remote Sensing Lett.*, **5**, 231-235.

Melnikov, V. et al., 2014: Doppler velocities at orthogonal polarizations in echoes from insects and birds. *IEEE Geosci. Remote Sensing Lett.*, **11**, 592-596.

Stepanian, P. M. et al., 2015: Extracting migrant flight orientation profiles using polarimetric radar. *IEEE Transactions on Geosci. And Remote Sensing*, **99**, 1-11.

Vaughn, C., 1985: Birds and insects as radar targets: a review. *Proc. IEEE* **73**, 205-227.